ACS APPLIED MATERIALS & INTERFACES

Research Article

www.acsami.org

In Vitro Investigation of Enhanced Hemocompatibility and Endothelial Cell Proliferation Associated with Quinone-Rich Polydopamine Coating

Rifang Luo,[†] Linlin Tang,[†] Si Zhong,[‡] Zhilu Yang,[†] Jin Wang,*[,†] Yajun Weng,[†] Qiufen Tu,[†] Chongxi Jiang,[†] and Nan Huang[†]

[†]Key Lab of Advanced Technology of Materials of Education Ministry and [‡]School of Life Science and Engineering, Southwest Jiaotong University, Chengdu 610031, China

Supporting Information

ABSTRACT: Recent investigations have demonstrated that polydopamine (PDA)-modified surfaces were beneficial to the proliferation of endothelial cells (ECs). In this work, PDA coated 316L stainless steels (316L SS) were thermally treated at 50, 100, and 150 °C respectively (hereafter designated as Th50, Th100, and Th150) and consequently produced diverse surface chemical components. In vitro hemocompatibility and vascular cell-material interactions with ECs and smooth muscle cells (SMCs) affected by surface characteristics have been investigated. The Th150, rich in quinone, showed the best hemocompatibility and could effectively inhibit platelet adhesion, activation, and fibrinogen conformation transition. The polydopamine-modified surfaces were found to induce dramatic cell-material interaction with enhanced ECs proliferation, viability and migration, release of nitric oxide (NO), and reduced SMCs proliferation. The inhibitory effect of SMCs proliferation might be associated with the surface catechol content. The coating on Th150 showed a good resistance to the deformation of compression and expansion of vascular stents. These results effectively suggested that the Th150 coating might be promising when served as a stent coating platform.

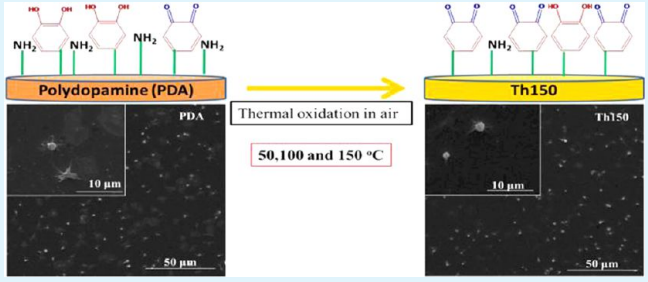

KEYWORDS: *polydopamine, surface modification, hemocompatibility, vascular stent, endothelialization, thermal*

INTRODUCTION

Many vascular interventional devices, such as stents and venacava filters which are made of stainless steels (SS), titanium, sharp memory nitinol, and cobalt-based alloy, have been widely applied to clinical treatment.[1,2] However, in response to acute vessel-wall injury caused by angioplasty, the increased incidence of thrombosis, restenosis, and fibromuscular proliferation[3,4] are not avoidable. As well accepted, the proliferation of vascular smooth muscle cells (SMCs) is principally responsible for in-stent restenosis and remains a challenging clinical problem. In recent years, the emerging of drug-eluting stents (DES) has resulted in suppressing neointimal hyperplasia and accordingly reducing in-stent restenosis rates.[5,6] However, a significant issue, late stent thrombosis, is one of the biggest challenges facing current DES because of the failure of re-endothelialization because of the inhibitory effect of the drug incorporated in stents on endothelial cells (ECs) during the drug eluting process.[7−9] It is therefore of significant importance that a desirable coronary stent should not only suppress inflammation and SMCs proliferation but also promote the proliferation of ECs. In-situ inducing re-endothelialization has also been highlighted in recent studies.[10−12]

One of the most important functions of ECs is to provide an inherent nonthrombogenic potential interface that protects the vasculature from pathological state like occlusion and neointimal formation after vascular surgery.[13−15] Thus, modulating the behavior of ECs such as adhesion, proliferation, migration, and differentiation is particularly important for endothelialization on artificial vascular grafts. Till now, numerous approaches of surface modification, including bioactive coatings,[16,17] immobilization of adhesive peptides (RGD),[18] and vascular endothelial growth factor (VEGF)[19] have been proposed to accelerate in situ inducing re-endothelialization of grafts by regulating cell-material interactions. These techniques to some extent enhanced ECs' adhesion and growth, but most were associated with poor anticoagulant properties. In our view, a potential solution for these problems is to develop a multifunctional interface which not only provides good hemocompatibility but also does well in modulating vascular cell-material interactions and effectively enforce the re-endothelialization process.

Received: November 20, 2012
Accepted: February 5, 2013
Published: February 5, 2013

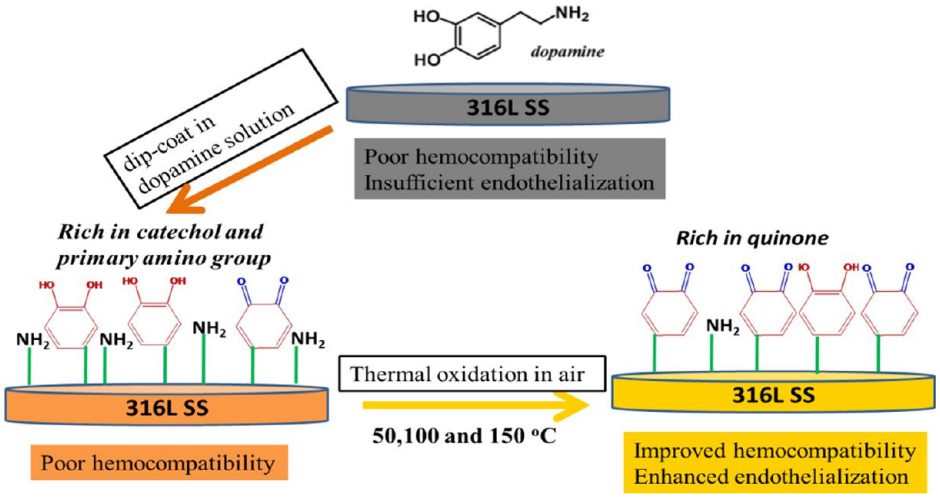

Figure 1. Scheme of 316L SS coated with polydopamine and the different chemical components and possible effect of polydopamine after thermal treatment.

Polydopamine (PDA), a bioinspired coating material, has the particular importance of providing an extremely versatile platform for secondary reactions by Schiff base or Michael additions, leading to tailoring of the coatings for diverse functional uses.[20,21] As an ad-layer, cell-material interactions affected by PDA-modified surfaces had been investigated recently. Ku and Park[22] found that ECs exhibited highly enhanced adhesion and viability when polycaprolactone (PCL) nanofiber scaffold was coated with PDA. Lynge et al.[23] found that PDA-coated glass substrate could support the adherence and proliferation of myoblast cells. Additionally, Lee et al.[24] recently published a result that the surface functionalized with PDA attenuated the in vivo toxicity (e.g., blood toxicity) and inflammatory responses to the implanted materials. These results suggested that PDA presented a potential application in surface modification of vascular biomaterials.

In previous work, we found that the PDA-coated 316L SS could enhance the attachment, proliferation, migration, and function of ECs. PDA coating had the ability to inhibit SMCs' adhesion and proliferation and thus might be able to address issues associated with re-endothelialization and restenosis.[25] It was speculated that the cellular behaviors of ECs and SMCs might be affected by the functional groups like primary amino, catechol, and quinone existing on the PDA surfaces. To elucidate this, 316L stainless steel (316L SS) was functionalized with PDA and then thermally treated in air for a facile oxidation of surface chemical groups. Particularly, for PDA which might be used in blood-contacting circumstance, the effect of surface chemical components on both hemocompatibility and the cellular behaviors of SMCs and ECs had never been systematically investigated to our knowledge. Therefore, this work aims at the systematic evaluations of hemocompatibility and the behaviors of SMCs/ECs affected by surface chemical components. The preparation of polydopamine and subsequent evaluations affected by diverse chemical components are illustrated in Figure 1.

EXPERIMENTAL SECTION

Materials. 316L stainless steel (SS) was obtained from New Material Co., Ltd. (Xi'an, China) and dopamine was purchased from Sigma-Aldrich (U.S.A.). Tris(hydroxymethyl) aminomethane (Tris-base) and glutaraldehyde were bought from Jinshan Chemical Reagent (Chengdu, China). Micro-BCA was obtained from Pierce Biotechnology Inc. (Rockford, U.S.A.). Various reagents used for the evaluation of hemocompatibility and cytocompatibility were provided from professional manufacturers which were mentioned in the Experimental Section. Other reagents were local products of analytical grade.

Preparation of Polydopamine Coatings. Dopamine solution was prepared by dissolving dopamine hydrochloride (2 mg/mL) in Tris-base buffer (10 mM, pH = 8.5). Mirror polished 316L SS (Φ = 10 mm) were then immersed in the above solution at 20 °C for 12 h. After that, polydopamine coated 316L SS were ultrasonically washed with double distilled water (10 min ×3 times). The above processes were repeated 3 times, and then the PDA coated 316L SS were placed in a drying cabinet, subsequently treated for 1 h at 50, 100, and 150 °C (hereafter labeled as Th50, Th100, and Th150, respectively).

Surface Characterization. The infrared spectra of all coatings were obtained between 4150 and 650 cm^{-1} using an attenuated total reflectance Fourier transform-infrared (ATR/FTIR, NICOLET 5700) spectrophotometer. The chemical composition was analyzed by X-ray photoelectron spectroscopy (XPS, Perkin-Elmer 16PC) with a monochromatic Al Kα excitation radiation ($h\nu$ = 1253.6 eV). Binding energies were calibrated by using the containment carbon (C1s = 284.7 eV). A Shirley background was used, and peaks were fitted using Xpspeak 4.1 to obtain the high resolution information. The contact angle was measured by static drops using DSA100 (Krüss, Hamburg, Germany) with the method depicted by the manufacturer at 25 °C and 60% relative humidity. Moreover, the surface energy was calculated by the method described by Owens and Wendt[26] with the data of the contact angle of water (polar solvent) and diiodomethane (nonpolar solvent).

Surface Quantification of Amine and Catechol. The QCM-D instrument (QCM-D, Q-Sense, AB, Göteborg, Sweden) was adopted for the relative quantification of the primary amine groups ($-NH_2$) of polydopamine coatings by a real-time monitoring of the Schiff base reaction between glutaraldehyde and the primary amine of polydopamine. Prior to the test, coatings were prepared on AT-cut 5 MHz Au-coated single crystal quartz (diameter of Au films: 10 mm). Each modified crystal was initially exposed to 20 mM PBS (pH = 7.3) fluid at 50 μL/min to remove unstable polydopamine. After that, a 2.5 wt % glutaraldehyde was then passed through the chamber in contact with the crystal. The frequency shift (Δf) was related to the adsorbed mass (Δm) according to the Sauerbrey relation.[27]

$$\Delta m = \Delta f \times C/n \quad (1)$$

C (C = 17.7 n g/cm^2 H Z^{-1} at f_n = 5 MHz) is the mass-sensitivity constant and n (n = 1, 3, 5, ...) is the overtone number.

The micro-BCA protein assay combines the well-known reduction of Cu^{2+} to Cu^{+} by proteins in an alkaline medium with the highly sensitive and selective colorimetric detection of the cuprous cation

(Cu^+) by bicinchoninic acid. Herein, a modified Micro-BCA method[28,29] was adopted because catechol of polydopamine could lead to the reduction of Cu^{2+} to Cu^+ and form the BCA/Cu^+ complex. The 160 μL of Micro-BCA working solution (A/B/C/sodium carbonate buffer = 25:24:1:50) was added to the surface of each sample and incubated at 37 °C for 1.5 h. Thus, the relative quantification of catechol could be achieved just according to the water-soluble BCA/Cu^+ complex which exhibited a strong linear absorbance at 562 nm.

In Vitro Hemocompatibility. The amounts of the samples used for statistical count were no less than five, and each test was carried out more than three times. The fresh human whole blood for the experiments was legally obtained from Blood Center of Chengdu, China. The analysis was performed within 8 h after the blood donation. The evaluations of hemocompatibility were illustrated in detail as the following parts. PDA, Th50, Th100, and Th150 surfaces were all tested for hemocompatibility and 316L SS was used as the control.

Morphology of Platelet Adhesion and Activation. Fresh human blood was centrifuged at 1500 rpm for 15 min to collect the top layer of platelet rich plasma (PRP). Afterward, 60 μL of PRP was added onto the sample surfaces placed in the 24-well plate and then incubated for 2 h at 37 °C. Then the samples were carefully rinsed with PBS solution to remove nonfirmly adsorbed platelets. After fixed with 2.5 wt % glutaraldehyde solution for 12 h, samples were washed with distilled water three times. The platelets adsorbed on the surfaces were dehydrated with 40, 50, 70, 90, and 100 vol % ethanol/water solution for 15 min each in sequence. After natural drying, the resultant samples were sputtered with gold, and then examined by scanning electron microscopy (SEM, Quanta 200, FEI,Holland).

Ratio of Adhered Platelets: Lactate Dehydrogenase (LDH) Assay. The platelet adhesion level of each polydopamine coated 316L SS was measured by the lactate dehydrogenase (LDH) released from the platelet lysed with a Triton-PSB buffer (2% v/v Triton-X-100 in PSB). PRP (60 μL) was added onto each surface of samples and incubated at 37 °C for 45 min. With the samples subsequently rinsed three times in PBS, 40 μL of Triton-X-100 (diluted to 1%) was added onto the surface. Then 5 min later, 25 μL of the lysates was taken from the surface and mixed with a substrate solution of 200 μL of NADH and sodium pyruvate in a 96-well plate. A calibration curve was constructed and the slope of the curve was evaluated and calibrated with lysates of all platelets at the absorbency of 340 nm.

Ratio of Activated Platelets: Assay of p-selectin (GMP-140). The ratio of activated platelets on the sample surface was determined using the assay of p-selectin GMP-140. Briefly, 60 μL of PRP was added onto each sample surface and incubated at 37 °C for 2 h. After being rinsed with PBS (pH = 7.5, 5 min ×3 times), 20 μL of anti-CD62p (GMP-140, MCA796GA, Serotec Co.) dilution at a final ratio of 1:100 was added onto each sample and incubated for 1 h at 37 °C. With PBS washed (5 min ×3 times), all the samples were incubated with 20 μL of horseradish peroxidase conjugated sheep anti mouse polyclonal antibody (second antibody, HRP, Catalog No: 074-1806, KPL Co.) at a dilution of 1:200 for 1 h at 37 °C. After washed with PBS (5 min ×3 times), 100 μL of 3, 3′, 5, 5′-tetramethylbenzidine (TMB) chromogenic solution was added to react with the second antibody for 10 min. By adding 50 μL of H_2SO_4 (1M), the reaction was stopped. And the optical density was examined using a microplate reader at the absorbance of 540 nm.

γ-Chain of Fibrinogen Exposure Evaluation. For the fibrinogen conformation transition test, fresh human blood was centrifuged at 3000 rpm for 15 min to obtain the platelet poor plasma (PPP). Each sample was incubated with 60 μL of PPP at 37 °C for 2 h. After that the samples were washed with PBS (5 min ×3 times). Subsequently, 20 μL of mouse anti human γ-fibrinogen monoclonal antibody (1:100 dilution, primary antibody, Product No: NYB4-2xl-f, Accurate Chemical & Scientific Corp) was added onto each sample and incubated at 37 °C for 1 h. After washing with PBS (5 min ×3 times), samples were incubated with 20 μL of HRP sheep anti mouse polyclonal antibody (second antibody, Catalog No: 074-1806, KPL Co.) solution (1:200 dilution) for 1 h at 37 °C. After three consecutive washes with PBS, the samples were reacted with 100 μL of chromogenic substrate TMB solution for 10 min. The color reaction was stopped by adding 50 μL of 1 M H_2SO_4, and the optical density was examined using microplate reader at 540 nm.

ECs Culture and Viability Assay. Human umbilical vein ECs (HUVECs) were isolated from newborn umbilical cord according to Jaffe et al.[30] using enzymatic digestion. Following isolation, HUVECs were cultured in M199 media (Gibco, U.S.A.) supplemented with 15% FBS (Sigma, U.S.). Cells were cultured in humidified air containing 5% CO_2 at 37 °C, and cells in passage 2 were used. To investigate the cell proliferation behavior affected by different sample surfaces, ECs were seeded at a concentration of 5×10^4 cells/per sample and incubated at 37 °C in 2 mL of M199 culture media supplemented with 15% FBS and 20 μg/mL endothelial cell growth supplement (ECGS). After the predetermined time points (2 h, 1 day, 3 day), samples were taken out, and the nonadherent cells were eliminated by PBS washing and the adherent cells were fixed with 2.5% glutaraldehyde for 4 h. After that, cells were Rhodamine-phalloidin stained (50 μL per sample, lucifuge for 20 min) and 4,6-diamidino-2-phenylindole dihydrochloride (DAPI) stained for nucleus (50 μL per sample, lucifuge for 10 min), respectively. After that samples were visualized by fluorescent microscopy (Zeiss, Germany). In brief, images were obtained and then processed using IPWin60C (software), and the average cell spreading area and cell number was then converted to evaluate the cell adhesion and proliferation. To investigate the endothelial cell metabolic activity (viability) on different samples, a colorimetric test based on a cell counting kit-8 (cck-8) assay was carried out. ECs were seeded onto each sample at 5×10^4 cells per well. After 1 day and 3 days culture, M199 media was removed and 400 μL of cck-8 (Dojindo, Japan) was added into each well and incubated for another 4 h to form water dissoluble formazan. Then 120 μL of the above formazan solution was taken out from each sample and added into one well of a 96-well plate. The optical density was measured at 450 nm wavelength with the microplate reader.

ECs Migration Test. The migration of ECs on different samples (n = 4) was carried out according our previous method.[25] Briefly, HUVECs were seeded onto the samples in the same way except that the cell density was varied to 5×10^5 cells/per sample to form a confluent monolayer after being cultured for 6 h. After that, the tip of a sterilized plastic pipet was used to scratch the confluent EC layer gently to create a scarification. Then the scarified samples were continuously cultured for another 2 days. After fixing and immunostaining, the samples were viewed via fluorescence microscope.

Nitric Oxide Release Test. For NO release detection, HUVECs with high density (5×10^5 cells/cm^2) were seeded onto each sample to make sure the formation of a confluent monolayer. After adhesion for 6 h, all the samples were transferred to new culture plates, and 1 mL of new culture medium was subsequently added. After being cultured for 24 h, 150 μL of the culture medium was collected. After being cultured for 2 days, 1 mL of the new culture medium replaced the original one and another 150 μL of culture medium was collected 24 h later. All the collected culture media were stored at −20 °C. NO release was indicated by the content of nitrite, which is a stable metabolite of NO. Nitrite was detected using Griess reagent (Sigma). In brief, collected culture media was centrifuged to remove all particulates at 800 rpm, and 100 μL of supernatant was injected into a new 96-well plate, and then an equal volume of Griess reagent was added. After that, the mixture was incubated at room temperature for 15 min and then was read at 540 nm using a microplate reader. Here, the quantification of NO release was ultimately divided by cell number.

SMCs Culture and Viability Assay. Human umbilical artery smooth muscle cells (HUASMCs) were isolated from newborn umbilical cord by the explant method as described previously.[31] Following isolation, SMCs were cultured in DMEM-F12 media (Gibco, U.S.A.) supplemented with 10% FBS (Sigma, U.S.). Cells were cultured in humidified air containing 5% CO_2 at 37 °C and cells in passage 2−5 were used. To investigate the cell proliferation behavior, SMCs were seeded at a density of 5×10^4 cells/per sample and incubated at 37 °C in DMEM-F12 media supplemented with 10% FBS

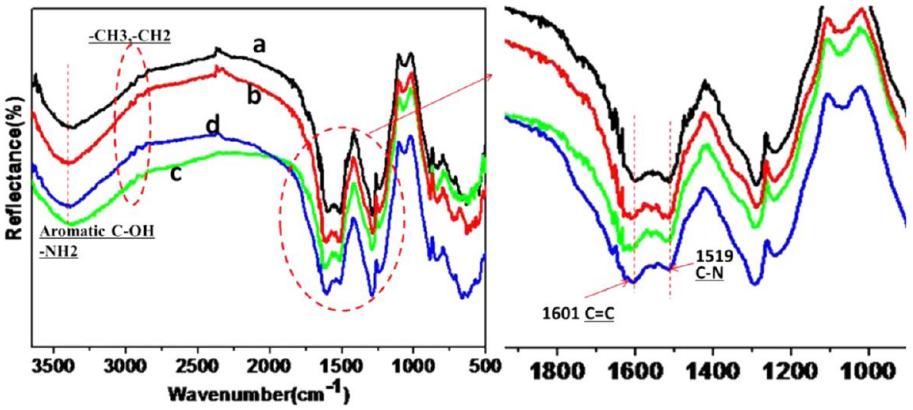

Figure 2. ATR-FTIR spectra of PDA (a), Th50 (b), Th100 (c), and Th150 (d).

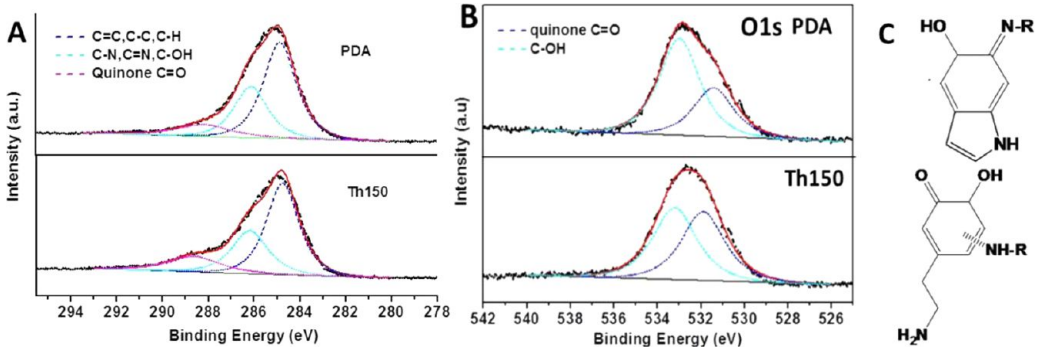

Figure 3. (A) Curve fitting results of C1s and O1s; (B) the spectra of PDA and Th150 modified surfaces; (C) the chemical bonding style existed on polydopamine modified surfaces.

for predetermined time points (1 day, 3 days). After each time point, samples were taken out and washed in PBS. Then all the samples were fixed, fluorescence stained, and visualized by fluorescent microscopy as the same procedure mentioned in ECs evaluation. Additionally, to investigate the viability of SMCs, cck-8 assay was also adopted with the same process mentioned above.

Morphology Examination and Balloon Expansion Tests. The surface morphologies of the expanded and nonexpanded 316L SS stents coated with PDA and Th150 were examined by SEM. A 1.65 × 18 mm 316L SS stent was mounted onto an angioplasty balloon and then the balloon was dilated from 1.65 to 3 mm (diameter) at a pressure of 8 atm. The maximum opening angle of the stents was examined.

Statistical Analysis. In this work, at least five samples per time point for each experimental condition were used. All the quantitative results were reported as mean ± standard deviation (SD). Statistical analysis was carried out by means of one-way analysis of variance (ANOVA). Statistically significance was accepted at the p-value less than or equal to 0.05 ($p \leq 0.05$).

RESULTS AND DISCUSSION

Because of the easy oxidation of catechol and amino structure, polydopamine coating could be thermally treated at a predetermined temperature to obtain different chemical components. On the basis of this tentative idea, the cellular behavior of ECs and SMCs affected by surface components could be evaluated. Additionally, of great importance is the assessment of hemocompatibility of polydopamine-modified surfaces which might potentially be applied in blood-contacting environments.

Chemical Components. The chemical structures of modified surfaces were analyzed by ATR-FTIR spectroscopy. As shown in Figure 2, all polydopamine coatings had a broad peak around 3400 cm^{-1} ascribed to aromatic -NHx and -OH stretching vibrations. The coatings also presented peaks at 2920 and 2850 cm^{-1} (aliphatic C−H stretching vibrations of CH_2), 1601 cm^{-1} (the overlap of C═C resonance vibrations in aromatic ring) and 1519 cm^{-1} (N−H scissoring vibrations). These are also in consistent with the reported results[32,33] and suggested that the 316L SS was successfully coated with polydopamine components. Interestingly, after thermal treatment, the peak at 1601 cm^{-1} was broad with enhanced intensity while the peak at 1519 cm^{-1} became narrower with reduced peak intensity. The distinct contrast could be seen in the Th150 compared to the PDA coating. According to the above results, it is speculated that, during thermal treatment, the polydopamine incurred intramolecular cyclization and formed indole derivatives which led to the enhanced peak intensity at 1601 cm^{-1} and the decreased peak intensity at 1519 cm^{-1}, as shown in Figure 3 C. Furthermore, the decrease in peak intensity at 1519 cm^{-1} might also be ascribed to the oxidation of a primary amino group under thermal condition.

Given that Schiff base reaction occurred, it seemed that the oxygen content decreased as a result of the substitution of oxygen by nitrogen. As shown in Table 1, some decrease in the oxygen content and an increase in the carbon content was detected at all polydopamine surfaces, compared with the original dopamine. However, when the thermal temperature was increased, a significant decrease/increase could be found in the nitrogen/oxygen content which was likely caused by the oxidation of primary amine groups. Moreover, the increase of the ratios of O/N and C/N suggested a possible production of carbamate caused by reaction of primary amine groups with water and carbon dioxide in air.[25]

dx.doi.org/10.1021/am3027635 | ACS Appl. Mater. Interfaces 2013, 5, 1704−1714

Table 1. Elemental Composition and Ratios of Dopamine (Theoretical Value) and of Each Polydopamine Coating As Determined by XPS

samples	C(%)	N(%)	O(%)	O/N	C/N
dopamine	72.7	9.1	18.2	2.0	8.0
PDA	76.6	7.5	15.9	2.1	10.2
Th50	75.5	7.2	17.3	2.4	10.5
Th100	75.6	6.2	18.2	2.9	12.2
Th150	75.0	5.9	19.1	3.2	12.7

To obtain the detailed chemical composition of each sample surface, further investigations of the C1s and O1s peak fittings were performed. The binding styles on polydopamine surface were complicated (Figure 3C) and referring to published fitting scheme,[25,34−37] C1s could be curve fitted into three main components by a best deconvolution. For example, according to Figure 3, C1s spectra of PDA and Th150 presented broad peaks: Part 1 (284.7 eV) was assigned as C═C, C−C, and C−H; Part 2 (286.1 eV) was assigned to C−N, C═N, and C−OH; Part 3 (288.3 eV) was ascribed to the quinone (C═O). The O1s core-level spectrum could be resolved into two typical peaks at 531.4 eV (quinone C═O) and 533.0 eV (catechol C−OH). Moreover, the components of total C1s and O1s of each surface were tested (Supporting Information, Table S1 and Table S2). Note that the PDA had 33.5% quinone content while the quinone content of Th150 increased to 48.2% according to the curve fitting result of O1s. Here, the Th150 coating was rich in quinone content.

Surface Hydrophilicity and Surface Energy. The water contact angle (WCA) of each sample is shown in Figure 4 A. Noteworthily, the original PDA presented a value of 65.4° while the WCA values of the thermally treated coatings increased with the increase of thermal temperature and reached 86.4° of Th150. Meanwhile, as shown in Figure 4 B, the surface energy also presented a systematic decrease with the increase of thermal temperature. The sharp decrease of polar surface energy indicated that the polar components in polydopamine, to some extent, disappeared or transformed to other less polar components (the polar surface energy of PDA was 11.2 mN/m while the polar surface energy of Th150 was 2.8 mN/m). As illustrated before, it might be ascribed to the decrease of the content of primary amino groups (hydrophilic group) which participated in the indole structure formation and oxidation and thus were consumed. Additionally, during thermal treatment, phenolic hydroxyl was oxidized to quinone which had lower polarity.

Quantitative Determination of Surface Functional Groups. The Micro-BCA method was used to form water-soluble BCA/Cu^{+} complex due to the catechol which could chelate cooper and lead to the reduction of Cu^{2+} to Cu^{+}. Because the catechol group had the reducibility, the results of this test could reflect the catechol content of different samples. According to the results shown in Figure 5 A, the OD value exhibited a systematic decrease with the increasing thermal temperature which was attributed to the catechol oxidation to quinone structure.

In addition, the real-time monitoring of the reacting of glutaraldehyde with polydopamine was investigated by QCM because the reacting dose could reflect the corresponding density of the surface primary amino group due to the Schiff base reaction. As shown in Figure 5 B, the glutaraldehyde reacting density of PDA reached up to 8.21 nmol/cm^2, and a remarkable reduction of reacting density was observed after being thermally treated merely at 50 °C (2.1 nmol/cm^2). Moreover, the density was extremely low in Th100 and Th150 (only about 1.2 nmol/cm^2 and 0.6 nmol/cm^2, respectively). In summary, Th150 modified surface was rich in quinones while poor in catechols and primary amino groups. Note that, relative quantification of functional group contents showed good agreement with the results of XPS, FTIR, and surface hydrophilicity analysis.

Hemocompatibility. Biomaterial-induced blood coagulation still remains a major obstacle which limits the successful use of implantable and peripheral medical devices.[33]Usually, rapid adsorption of plasma proteins occurs after implantation, leading to platelet adhesion which triggers the coagulation of blood and thus the thrombus formation.[38] It is generally accepted that hemocompatibility depends on surface characteristics, including hydrophilicity/hydrophobicity and charge, influencing protein adsorption during the initial response to material−blood contact.[39] According to recent decades of research, the conformation of absorbed fibrinogen is considered to be a key factor in dealing with coagulation processes. Therefore, to better understand the hemocompatibility of polydopamine, platelet adhesion/activation and fibrinogen conformation change are investigated, associated with the evaluation of surface characteristics of different polydopamine. Hereon, the material-blood interaction is studied by an in vitro platelet adhesion test and ELISA assays (including LDH, GMP-140 and fibrinogen conformation transition).

According to Figure 6, the platelets adhered onto PDA and Th50 were almost fully spread, which indicated a high degree of platelet activation. However, on the surface of Th150, the shape of platelets still remained dendritic or even round which revealed that the activation of platelet was remarkably reduced by thermal treatment. The results of LDH and GMP-140 assays (Supporting Information, Figure S1) showed that the PDA coated surfaces, to a certain extent, enlarged the ratio of

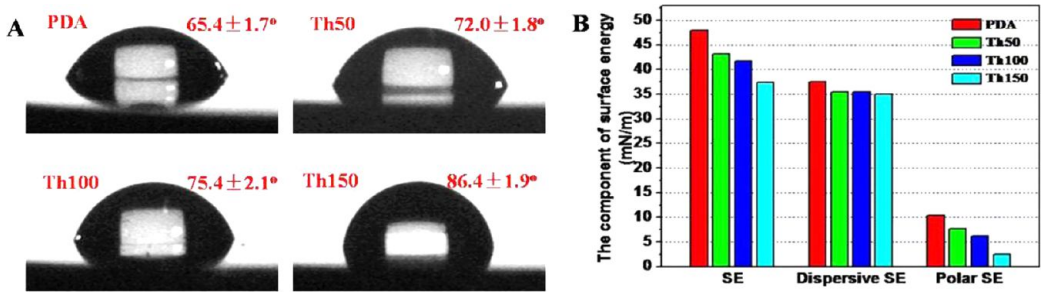

Figure 4. (A) Water contact angle and (B) surface energy of different polydopamine samples. (SE: surface energy, n = 5).

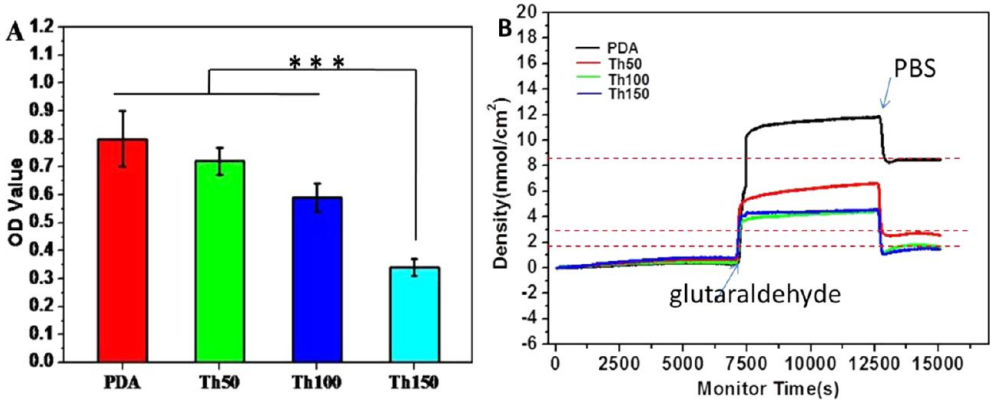

Figure 5. (A) Relative surface catechol content of each polydopamine determined via a modified micro-BCA measurement (n = 5, ***p < 0.001) and (B) relative primary amino group density of different polydopamines (reflected by glutaraldehyde reacting dose) determined by QCM measurement.

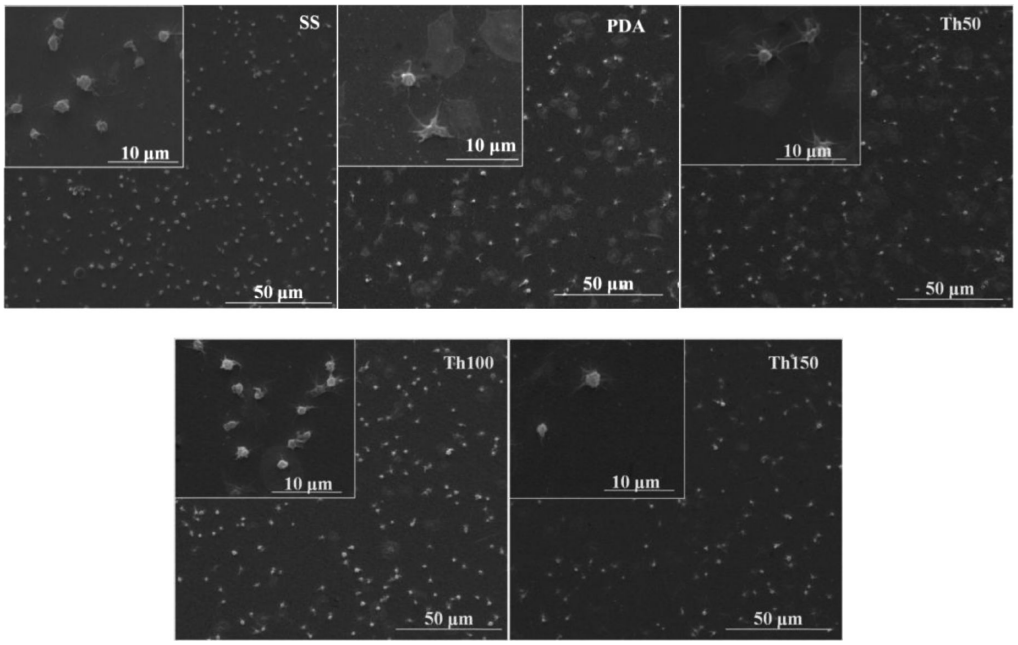

Figure 6. Morphology of adherent platelets on the surfaces of different polydopamine coating (2 h incubation in PRP) observed by SEM.

adhered and activated platelets as compared to 316L SS. Additionally, it could be found that the amount of adherent and activated platelets was least on the Th150 surface compared to other tested surfaces.

Compared with 316L SS, the ratios of platelet adhesion and activation on the PDA modified surface were higher which might be contributed by the large amount of primary amino groups (positively charged) that likely promote platelet adhesion (negatively charged) by electrostatic interaction.[40] Moreover, of great importance is the ability to inhibit the conformation change of fibrinogen. It was found that the PDA modified surfaces presented similar effect on fibrinogen conformation change compared to 316L SS which is widely used as a blood-contacting material in vascular stents and grafts. Lee et al.[21] reported that the catalytic activity of immobilized enzymes was fully retained on the polydopamine layers, indicating that no alteration in protein structure was caused by polydopamine. Ku et al.[37] suggested that polydopamine can be a versatile surface modifier that can minimize the denaturation of serum proteins by adjusting the surface energy of materials. Interestingly, the Th150 surface here presented the best ability in maintaining the fibrinogen conformation according to Figure 7. To better understand this, we also

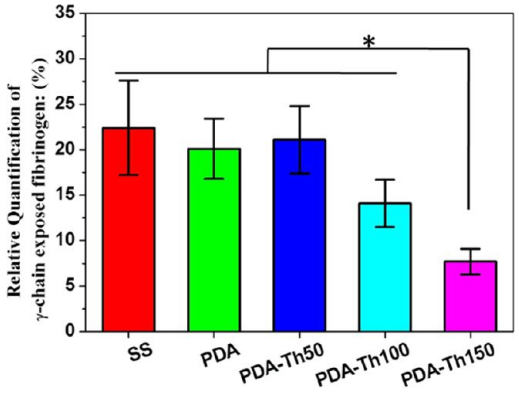

Figure 7. Relative quantification of γ-chain of fibrinogen exposure obtained by ELISA assays. Data expressed as mean ± SD (*p < 0.05).

dx.doi.org/10.1021/am3027635 | ACS Appl. Mater. Interfaces 2013, 5, 1704−1714

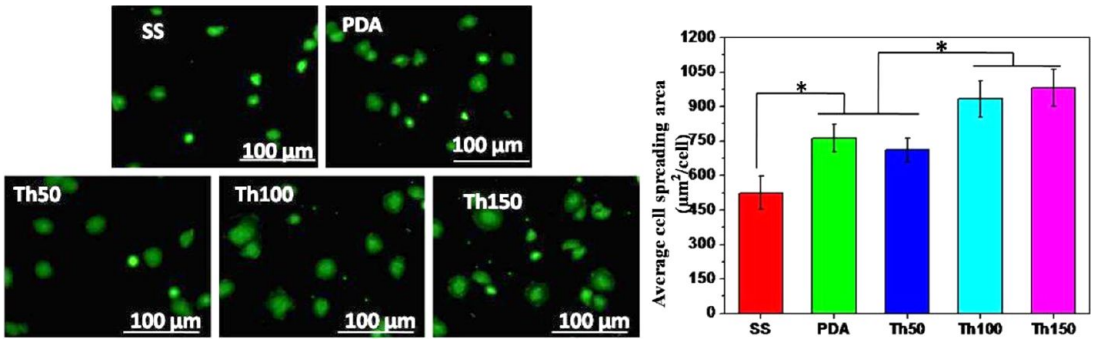

Figure 8. Cytoskeletal actin stains of ECs on the 316L SS and polydopamine modified surfaces after being cultured for 2 h (left), and the average cell spreading area of ECs adhered on each sample after culture for 2 h (right). Data presented as mean ± SD and analyzed using a one-way ANOVA, $*p < 0.05$.

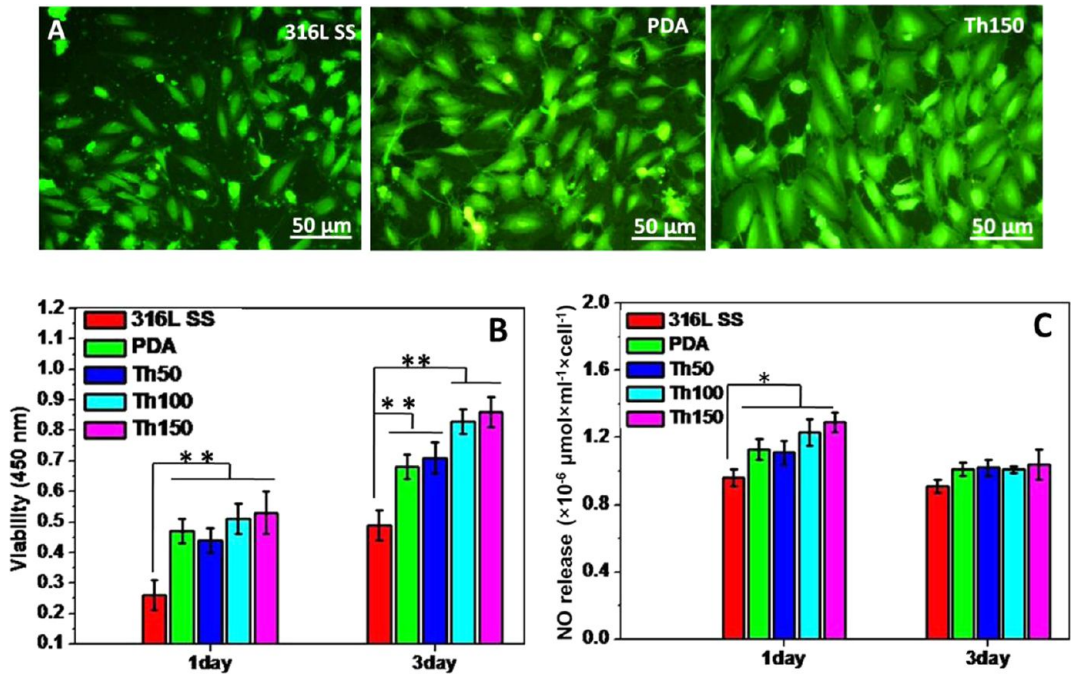

Figure 9. (A) Cytoskeletal actin stains of ECs on the 316L SS, PDA and Th150 surfaces after 3 days of culture; (B) The viability of ECs attached onto 316L SS and different polydopamine modified surfaces after cultures of 1 and 3 days; (C) NO levels released in the culture media (the size of sample: Φ18 mm, $n = 4$). Data presented as mean ± SD and analyzed using a one-way ANOVA, $*p < 0.05$, $**p < 0.01$.

monitored the adsorption behavior of bovine serum albumin (BSA) and bovine fibrinogen onto the PDA and Th150 surfaces with the help of QCM measurement (Supporting Information, Figure S2). After thermal treatment, the Th150 surface was more potent in the adsorption of BSA (almost 680 ng/cm^2) compared with the PDA surface (about 300 ng/cm^2). However, no significant differences could be found in the fibrinogen adsorption test (100 and 115 ng/cm^2 onto PDA and Th150 surface, respectively). We speculated that Th150 surface might be beneficial to the preferential absorption of albumin, which induced better anticoagulant properties. However, further work is urgently needed to investigate the mechanisms involved in the interaction of blood components with polydopamine components. Nevertheless, this work suggested that the Th150 surface, poor in amino groups and rich in quinone, was beneficial to maintain the natural conformation of fibrinogen, which thereby inhibited platelet adhesion and activation. These results also effectively implied that Th150 coating might be a promising blood-contacting interface in surface modification.

Adhesion, Proliferation, and Migration of ECs. Of great importance is to understand how ECs interact with foreign materials and rapid re-endothelialization had been frequently demonstrated in the survival of implants.[10−12] As reported by Ku et al.,[37] the enhanced ECs' adhesion on polydopamine-modified PCL nanofibers might be attributed to the serum protein adsorption/immobilization which could effectively maintain their natural properties. As a versatile modifier which might be used in blood-contacting materials, in our view, the polydopamine surface would possibly react with the serum proteins containing amine- or thiol- functional groups at the initial prime and thus become the cell adhesion site. Thus, to understand the proliferation behavior and function of ECs, the PDA and thermally treated PDA were adopted for the further investigation on ECs' morphology, proliferation, and functions. 316L SS was used as the control.

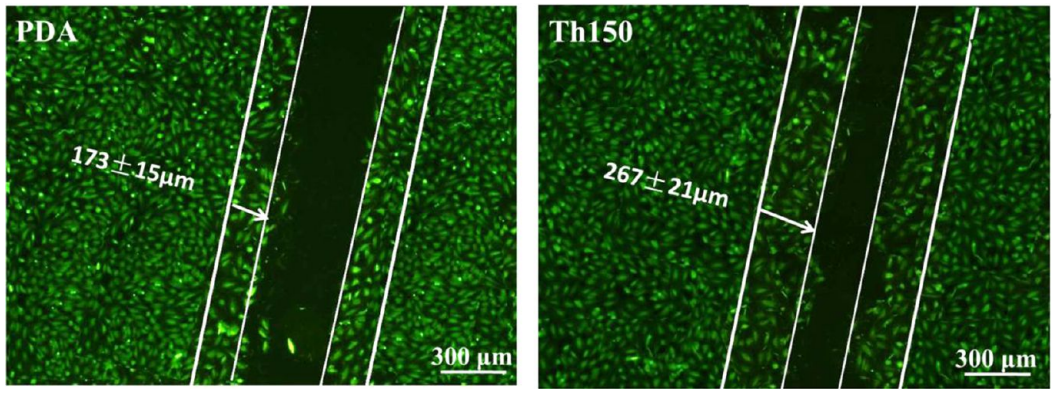

Figure 10. Migration of ECs on PDA and Th150 modified surfaces.

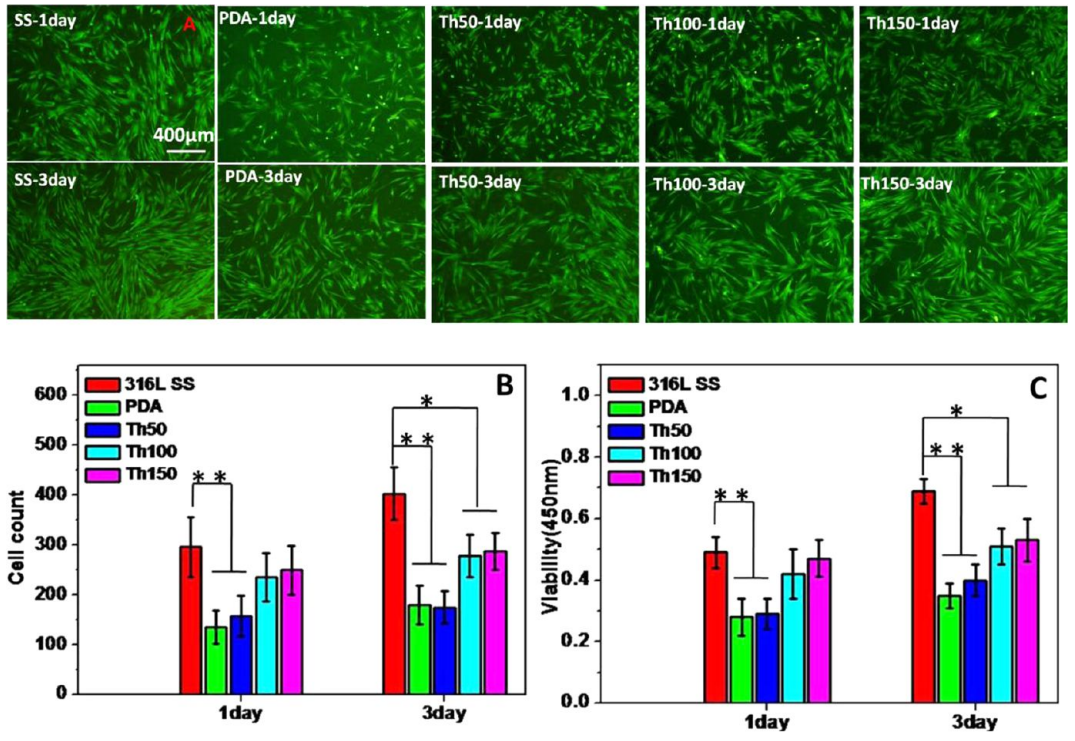

Figure 11. (A) Cytoskeletal actin stains, (B) cell count, and (C) cell viability (obtained by cck-8 assay) of SMCs on the 316L SS and different polydopamine modified surfaces after 1 day and 3 days culture.

As is well accepted, good cell adhesion property does a great favor in cell survival. The morphology of adhered ECs after 2 h culture was distinctly listed in Figure 8. Compared to 316L SS, the number of adhered ECs on polydopamine modified surfaces was higher, especially on Th100 and Th150 surfaces. Moreover, ECs on Th100 and Th150 surfaces had the larger cell spreading area, suggesting good focal adhesion formation which could not be found on 316L SS surfaces. Here, the proliferation and viability of ECs affected by samples was also presented (Supporting Information, Figure S3 A and B). The number of attached ECs on the samples generally increased during cell culture, and ECs on PDA modified surfaces presented higher cell viability. After being cultured for 1 day and 3 days, ECs presented proliferation rates of 28.5%, 39.6%, 38.1%, 45.3% and 47.3% on the 316L SS, PDA, Th50, Th100, and Th150 surfaces, respectively. Especially for the Th100 and Th150 surfaces, the results indicated that ECs were energetic in proliferation. Moreover, these surfaces could provide adequate conditions for cell to cell communication and EC monolayer formation. As reported by Anselme,[41] the cells adhered onto foreign materials by undergoing general cell adhesion processes like substrate attachment, spreading, and cytoskeleton development. In view of this, the relative hydrophilicity of PDA (with primary amino groups) facilitated quick attachment of ECs, subsequent cell spreading, and cytoskeleton development after a 1 day culture. Moreover, the surfaces of Th100 and Th150 contained higher content of quinone and had better secondary reactivity with serum proteins. It was speculated that Th100 and Th150 surfaces had better potentiality in interacting with serum proteins (adsorption or immobilization) and thus formed proper cell adhesion sites, leading to rapid cell proliferation. Cells cultured on Th150 surfaces also presented booming cell attachment and might imply strong extracellular matrix production and cell proliferation (Figure 9 A and B). Our previous study had shown that the polydopamine surface showed increased migration rate than the 316 L SS surface.[25]

dx.doi.org/10.1021/am3027635 | ACS Appl. Mater. Interfaces 2013, 5, 1704−1714

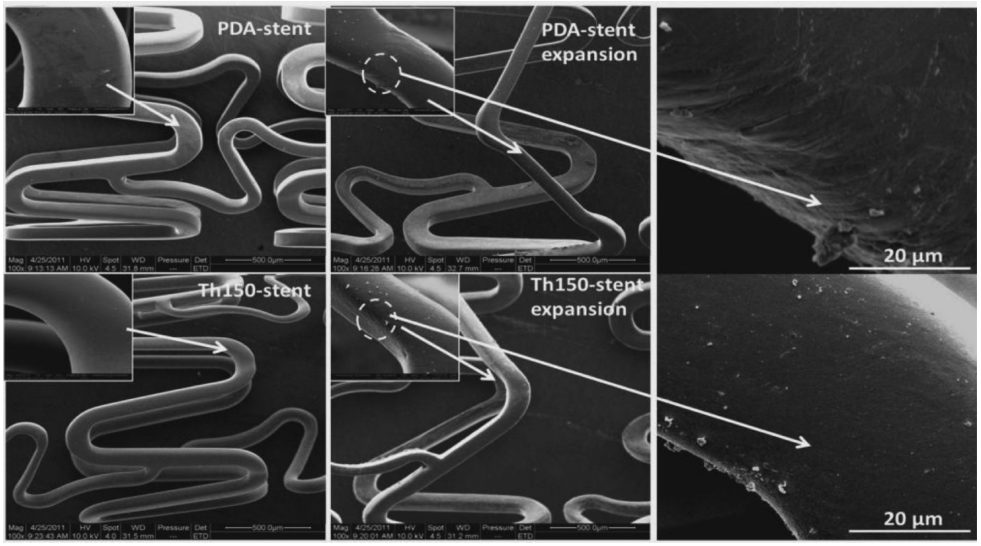

Figure 12. SEM micrographs of the 316L SS stents coated with PDA and Th150 about pre-expansion and postdilation image (Up) and Th150 (Down).

Hereon, according to Figure 10, the migration distance of cells seeded on the PDA surface was 173 ± 15 μm, while a visible increased migration distance of 261 ± 21 μm was obtained on the Th150 surfaces. These results also confirmed that the cells cultured on Th150 surfaces were more energetic.

In addition, further investigations of NO levels released in the culture media were carried out (Figure 9 C). As well accepted, natural ECs can provide an inherent nonthrombogenic potential interface via maintained vascular homeostasis by continuous release of NO which is a predominant product that acts as antithrombogenic and antiproliferative agent in SMCs. It was noteworthy that, after ECs were cultured for 1 day, the polydopamine modified surfaces, especially Th150, induced higher NO release level compared to 316L SS. Although NO levels released in the culture media somewhat decreased with the increase of culture time of cells, the polydopamine-modified surfaces still presented a higher NO level than 316L SS. Thus, the enhancement of NO release was a desirable quality after implantation of a foreign material because of the ability of inhibiting platelet adhesion, aggregation, and also SMCs' proliferation.

Proliferation and Viability of SMCs. As is well accepted, the proliferation of vascular smooth muscle cells (VSMCs) is principally responsible for in-stent restenosis and remains a challenging clinical problem in the treatment of vascular diseases.[4] Further investigations of SMCs' response to polydopamine affected by chemical components were first carried out here. As shown in Figure 11, after being cultured for 1 day, compared to the 316L SS surface, SMCs were more isolated on the PDA and Th50 surfaces. Moreover, SMCs presented a rapid proliferation rate on 316L SS during culture which could not be found on the polydopamine modified surfaces. After being cultured for 3 days, all the polydopamine modified samples presented significantly lower cell numbers and viability of SMCs, compared with 316L SS. These results strongly suggested that polydopamine did show significant inhibitive effects on the proliferation of SMCs.

In this work, polydopamine surfaces were thermally treated and led to different chemical components. The catechol content of PDA decreased with the increase of treating temperature. It was noteworthy that after culture for 1 day and 3 days, the viability of SMCs was the lowest on the PDA modified surface but the highest on the Th150 modified surface. Thus, it was speculated that the SMCs' behavior might be strongly associated with the surface catechol content. Chen et al.[42] found that purified green tea epicatechins had remarkably antiproliferative effect on rat arterial SMCs, and the phenolic groups were the key factor to influence SMCs proliferation. Briefly, based on reported results, polyphenols like (-)-Epigallocatechin-3-gallate (EGCG), (-)-epicatechin-3-gallate (ECG), and gallic acid (GA) could inhibit SMCs' adhesion and migration or even induce apoptosis via different approaches, including inhibiting the activation of pro-matrix metalloproteinase (MMP)-2 and the activities of membrane type 1-MMP(MT1-MMP),[43] down modulating nuclear factor-κB (NF- κB) expression,[44] inducing the expression of p53,[45] affecting SMC's integrin β1 expression and the binding to extracellular matrix (ECM) proteins.[46] Moreover, the inhibitory effects were associated with the dose of polyphenols in these reports. Additionally, GA could induce apoptosis of many types of cells, which might be associated with oxidative stresses derived from reactive oxygen species (ROS), mitochondrial dysfunction, and an increase in intracellular Ca^{2+} level.[47] However, no cytotoxicity against normal endothelial and fibroblast cells was found after GA treatment.[48,49] Involving polydopamine coating, a catechol containing material, which might also present a similar effect via its catechol oxidation (inducing ROS), binding SMCs' ECM proteins and thus affect integrin expression. However, until now the interaction mechanism between polyphenols and SMCs is still not quite clear. Further work about how the catechol of polydopamine affects SMC growth is urgently needed. Nevertheless, these results did imply that polydopamine might be promising when used as a coating for stents or vascular grafts.

Morphology Examination and Balloon Expansion Tests. A stent will suffer rigorous and complex distortion when it is mounted onto an angioplasty balloon and is dilated to 3.0 mm at a pressure of 8 atm. To actually understand the mechanical behaviors of PDA and Th150 as a stent coating, the expansion analysis of 316L SS stent coated with PDA and Th150 was thereby performed. As seen in Figure 12, Th150 coatings smoothed the surface of bare stents and could keep

intact with neither cracks nor webbings after balloon expansion compared with the PDA coated bare stents (coating stripped and slipped). This revealed that the Th150 coating was sufficiently flexible to adapt itself to synchronous deformation of the 316L SS that allowed balloon expansion of the stent without cracking or peeling from the struts.

CONCLUSION

We aimed at developing a multifunctional interface which not only provides good hemocompatibility but also functions well in inducing desirable vascular cell-material interaction. In this work, polydopamine with different chemical components was successfully prepared via a simple thermal oxidation of polydopamine modified 316L SS. It was found that, Th150 coating, rich in quinone content, showed the best hemocompatibility and was energetic in promoting EC proliferation and migration. Moreover, a polydopamine surface that could effectively inhibit SMC proliferation might be associated with the surface catechol content. Because of these properties, polydopamine surfaces might be able to address the issues associated with re-endothelialization and restenosis. Although remarkable and desirable effects on growth behavior of ECs and SMCs were obtained on polydopamine modified 316L SS, further investigations of details are urgently needed. Briefly, our work suggested that quinone-rich polydopamine (Th150) coating might provide a promising potential platform in surface modification on stents or vascular grafts.

ASSOCIATED CONTENT

Supporting Information

Table S1 and S2 for the components of total C1s and O1s of different polydopamines; LDH assay, GMP-140 assay and QCM-D measurement for protein adsorption; Endothelial cell proliferation result. This material is available free of charge via the Internet at http://pubs.acs.org.

AUTHOR INFORMATION

Corresponding Author

*Phone: +86 28 87634148. Fax: +86 28 87600625. E-mail: address:jinxxwang@263.net.

Notes

The authors declare no competing financial interest.

ACKNOWLEDGMENTS

This work is supported by National Natural Science Foundation of China (Project 51173149), Ministry of Scientific and Technical Project of China (Key Basic Research Project No. 2011CB606204), Natural Science Foundation for the Youth of China (Grant No. 31000426 and 30900295), and Fundamental Research Funds for the Central Universities (Grant No. SWJTU11CX057).

REFERENCES

(1) Williams, D. F. *Biomaterials* **2008**, *29*, 2941−2953.
(2) Mani, G.; Feldman, M. D.; Patel, D.; Agrawal, C. M. *Biomaterials* **2007**, *28*, 1689−1710.
(3) Lau, K. W.; Mak, K. H.; Hung, J. S.; Sigwart, U. *Am. Heart J.* **2004**, *147*, 764−773.
(4) Toutouzas, K.; Colombo, A.; Stefanadis, C. *Eur. Heart J.* **2004**, *25*, 1679−1687.
(5) Shaulov, Y.; Okner, R.; Levi, Y.; Tal, N.; Gutkin, V.; Mandler, D.; Domb, A. J. *ACS Appl. Mater. Interfaces* **2009**, *1*, 2519−2528.
(6) Garg, G.; Serruys, P. W. *Expert Rev. Cardiovasc. Ther.* **2010**, *8*, 449−470.
(7) Maisel, W. H. *N. Engl. J. Med.* **2007**, *356*, 981−984.
(8) Joner, M.; Nakazawa, G.; Finn, A. V.; Quee, S. C.; Coleman, L.; Acampado, E. *J. Am. Coll. Cardiol.* **2008**, *52*, 333−342.
(9) Finn, A. V.; Nakazawa, G.; Joner, M.; Kolodgie, F. D.; Mont, E. K.; Gold, H. K.; Virmani, R. *Arterioscler., Thromb., Vasc. Biol.* **2007**, *27*, 1500−1510.
(10) Li, G. C.; Yang, P.; Qin, W.; Maitz, M. F.; Zhou, S.; Huang, N. *Biomaterials* **2011**, *32*, 4691−4703.
(11) Meng, S.; Liu, Z.; Shen, L.; Guo, Z.; Chou, L. L.; Zhong, W. *Biomaterials* **2009**, *30*, 2276−2283.
(12) Yin, M.; Yuan, Y.; Liu, C. S.; Wang, J. *Biomaterials* **2009**, *30*, 2764−2773.
(13) Moncada, S.; Radomski, M. W.; Palmer, R. M. J. *Biochem. Pharmacol.* **1988**, *37*, 2495−2501.
(14) Weng, Y. J.; Song, Q.; Zhou, Y. J.; Zhang, L. P.; Wang, J.; Chen, J. Y.; et al. *Biomaterials* **2011**, *32*, 1253−1263.
(15) Ramamurthi, A.; Robson, S. C.; Lewis, R. S. *Thromb. Res.* **2001**, *102*, 331−341.
(16) Meyers, S. R.; Kenan, D. J.; Khoo, X. J.; Grinstaff, M. W. *Biomacromolecules* **2011**, *12*, 533−539.
(17) Adali, M. A.; Ziemer, G.; Wendel, H. P. *Biotechnol. Adv.* **2010**, *28*, 119−129.
(18) Chung, T. W.; Lu, Y. F.; Wang, S. S.; Lin, Y. S.; Chu, S. H. *Biomaterials* **2002**, *23*, 4803−4809.
(19) Zisch, A. H.; Schenk, U.; Schense, J. C.; Sakiyama-Elbert, S. E.; Hubbell, J. A. *J. Controlled Release* **2001**, *72*, 101−113.
(20) Lee, H.; Dellatore, S. M.; Miller, W. M.; Messersmith, P. B. *Science* **2007**, *318*, 426−430.
(21) Lee, H.; Rho, J.; Messersmith, P. B. *Adv. Mater.* **2008**, *20*, 1−4.
(22) Ku, S. H.; Park, C. B. *Biomaterials* **2010**, *31*, 9431−9437.
(23) Lynge, M. E.; Ogaki, R.; Laursen, A. O.; Lovmand, J.; Sutherland, D. S.; Städler, B. *ACS Appl. Mater. Interfaces* **2011**, *3*, 2142−2147.
(24) Hong, S.; Kim, K. Y.; Wook, H. J.; Park, S. Y.; Lee, K. D.; Lee, D. Y.; Lee, H. *Nanomedicine* **2011**, *6*, 793−801.
(25) Yang, Z.; Tu, Q.; Zhu, Z.; Luo, R.; Li, X.; Xie, Y.; Maitz, M. F.; Wang, J.; Huang, N. *Adv. Healthcare Mater.* **2012**, *1*, 548−559.
(26) Owens, D. K.; Wendt, R. C. *J. Appl. Polym. Sci.* **1969**, *13*, 1741−1747.
(27) Sauerbrey, G. *Z. Physik* **1959**, *155*, 206−222.
(28) Shin, Y. M.; Lee, Y. B.; Shin, H. *Colloids Surf. B* **2011**, *87*, 79−87.
(29) Slocum, T. L.; Deupree, J. D. *Anal. Biochem.* **1991**, *195*, 14−17.
(30) Jaffe, E. A.; Nachman, R. L.; Becker, C. G.; Minick, C. R. *J. Clin. Invest.* **1973**, *52*, 2745−2756.
(31) Vadiveloo, P. K.; Stanton, H. R.; Cochran, F. W.; Hamilton, J. A. *Artery* **1994**, *21*, 161−181.
(32) Zhu, L.; Jiang, J.; Zhu, B.; Xu, Y. *Colloids Surf. B* **2011**, *86*, 111−118.
(33) Guo, Z.; Bussard, K.; Chatterjee, K.; Miller, R.; Vogler, E. A.; Siedlecki, C. A. *Biomaterials* **2006**, *27*, 796−806.
(34) Xu, L.; Yang, W.; Neoh, K. G.; Kang, E. T.; Fu, G. *Macromolecules* **2010**, *43*, 8336−8339.
(35) Zhu, L.; Yu, J.; Xu, Y.; Xi, Z.; Zhu, B. *Colloids Surf. B* **2009**, *69*, 152−155.
(36) Jiang, J.; Zhu, L.; Li, X.; Xu, Y.; Zhu, B. *J. Membr. Sci.* **2010**, *364*, 194−202.
(37) Ku, S. H.; Ryu, J.; Hong, S. K.; Lee, H.; Park, C. B. *Biomaterials* **2010**, *31*, 2535−2541.
(38) Davie, E. W.; Fujikawa, K. *Annu. Rev. Biochem.* **1975**, *44*, 799−829.
(39) Sperling, C.; Fischer, M.; Maitz, M. F.; Werner, C. *Biomaterials* **2009**, *30*, 4447−4456.
(40) Yang, Z.; Wang, J.; Luo, R.; Maitz, M. F.; Jing, F.; Sun, H.; Huang, N. *Biomaterials* **2010**, *31*, 2072−2083.
(41) Anselme, K. *Biomaterials* **2000**, *21*, 667−681.

(42) Chen, Z. Y.; Law, W. L.; Yao, X. Q.; Lau, C. W.; HO, W. K. K.; Huang, Y. *Acta Pharmacol. Sin.* **2000**, *21*, 835−840.
(43) Cheng, X. W.; Kuzuya, M.; Nakamura, K.; Liu, Z.; Di, Q.; Hasegawa, J.; et al. *Arterioscler., Thromb., Vasc. Biol.* **2005**, *25*, 1864−1870.
(44) Han, D. W.; Lim, H. R.; Baek, H. S.; Lee, M. H.; Lee, S. J.; Hyon, S. H.; Park, J. C. *Biochem. Biophys. Res. Commun.* **2006**, *345*, 148−155.
(45) Hofmann, C. S.; Sonenshein, G. E. *FASEB J.* **2003**, *Apr;17*, 702−704.
(46) Lo, H. M.; Hung, C. F.; Huang, Y. Y.; Wu, W. B. *J. Biomed. Sci.* **2007**, *14*, 637−645.
(47) Chen, H. M.; Wu, Y. C.; Chia, Y. C.; Chang, F. R.; Hsu, H .K.; Hsieh, Y. C. *Cancer Lett.* **2009**, *286*, 161−171.
(48) Inoue, M.; Suzuki, R.; Koide, T.; Sakaguchi, N.; Ogihara, Y.; Yabu, Y. *Biochem. Biophys. Res. Commun.* **1994**, *204*, 898−904.
(49) Inoue, M.; Suzuki, R.; Sakaguchi, N.; Li, Z.; Takeda, T.; Ogihara, Y. *Biol. Pharm. Bull.* **1995**, *18*, 1526−1530.